Theoretical and Experimental Investigation of Ultrasonic Focusing with Annular Phased Array *

ZHANG Bi-Xing(张碧星)**, WANG Cheng-Hao(汪承灏), LAI Pu-Xiang(赖溥祥)
Institute of Acoustics, Chinese Academy of Sciences, Beijing 100080

(Received 29 November 2005)

The focused acoustic field generated by an annular array transducer and its reflection field on a solid–liquid interface are investigated theoretically and experimentally. Theoretically, the concise analytic expressions about the radiation and reflection acoustic fields of the annular phased array are obtained by the ray approach method (saddle-point method). In experiment, an annular transducer with 8 equal-area elements is designed and fabricated, and a series of experiments about the radiation acoustic field and its reflection on the liquid-solid interface are carried out. The experimental characteristics of the transducer are in good agreement with the numerical ones. It shows the correctness of the theoretical result and the feasibility of dynamic focusing of the experiment system. With the maximum amplitude and its emergence time of the reflection wave, we can acquire the information and the imaging of the reflection interface by the annular phased array dynamic focusing.

PACS: 43. 35. +d, 43. 58. +z

Ultrasonic phased array testing can accomplish dynamic focusing and the inspection of workpieces with complex geometry. Also, it can greatly improve the detection sensitivity, resolution and SNR, which lead to its high recognition in NDT research domain. The most frequently used phased arrays nowadays are linear phased arrays, two-dimensional (2D) phased arrays and annular phased arrays. Annular arrays have been somewhat overlooked, compared with the others. The main reason for this is that annular arrays are axially symmetric and they can only focus on the axial direction, which make it necessary to mechanically scan an annular array to form a 2D image.[1] However, annular arrays can form a high quality radiation focusing pattern with far fewer elements. This reduces greatly the cost of the transducer and the technology difficulties associated with developing transducers, and this simplifies the circuits and control system.[2] In many medical and NDT applications, useful information is acquired with the reflection waves on the interface of two media. In previous studies, a great deal of attention was paid to the acoustic radiation field of the annular phased array transducers. However, few authors studied the reflection of the focused field of a phased array on a solid–liquid interface. In this Letter, we investigate the reflection on a solid–liquid plane of the focused acoustic field excited by an annular phased array.

This study can be used in other applications of acoustic borehole televiewers (BHTVs).[3] In acoustic BHTVs about petroleum logging, the ultrasonic transducer, which rotates along the borehole axis, transmits the acoustical pulse to the borehole wall that is a solid–liquid interface and then receives the reflection signal. The variation of the borehole radius and the formation character can be extracted from the propagation time and the amplitude of the received signal. For the present acoustic BHTVs, the transducer is a concave or a plane piston. The focus of this kind transducer is fixed and cannot be adjusted dynamically. Thus, the testing result of BHTVs is not good for the boreholes whose radius varies significantly along the borehole axis, and different transducers should be adopted for the boreholes with different radii in practice applications. If the annular phased array is used to BHTV transducers, the focus could be changed dynamically by electrical manners. The transducers can be applied to the boreholes with different radii and the boreholes whose radius varies significantly. However, the annular phased array is yet not applied to BHTV instruments in practice because the theoretical study is not perfect.

Consider an ultrasonic array composed of N homocentric annular piezoelectric discs that are marked by number $1, 2, \cdots, N$ from inner to outer. The inner and outer radii of the jth annular array element are a_{2j-1} and a_{2j}, respectively. Define a cylindrical coordinate system centred at the centre of the annular array and oriented along the symmetric axis of the array. Each element vibrates along the z direction when they work.

The annular array is excited in liquid medium. The acoustical waves from each element to the field point have different propagation times and cannot coherently strengthen. If we hope that the waves from each element arrive at a given point M on the z axis in phase, each element should be excited with different original phases. When it is accomplished according to this sense, the annular phased array is realized and the field is focused at the point M that is called the focus. This time, the focused radiation field can be written as[4]

$$\psi = ik \sum_{j=1}^{N} e^{-i\Delta\phi_j} \iint_{s_j} ds \int_0^{(\pi/2-i\infty)} J_0(kr_1 \sin\theta) \cdot e^{ik|z_0 - z|\cos\theta} \sin\theta d\theta, \quad (1)$$

* Supported by the National Natural Science Foundation of China under Grant No 10134020.
** Email: zhbx@mail.ioa.ac.cn
©2006 Chinese Physical Society and IOP Publishing Ltd

where $r_1 = \sqrt{r^2 + r_0^2 - 2rr_0\cos(\theta_0 - \varphi)}$; (r, φ, z) and (r_0, θ_0, z_0) are the coordinates of the field point and source point; $\Delta\phi_j$ is the phase delay of the jth element and determined by the focus position; and k is the wavenumber in liquid media. The integration area s_j for s is on the surface of the jth element.

It is inconvenient to calculate the radiation field by Eq. (1) in numerical simulation. For this reason, the approximation representation for the radiation far-field (the distance from the field point to the transducer is much greater than the wavelength) of the annular phased array has been given by the ray approach method and can be written as the following form in the frequency domain,[5−9]

$$\psi = i\omega\rho_0 u_a \frac{e^{ikr_a}}{r_a} \sum_j^N \left[a_{2j}^2 \cdot \frac{J_1(ka_{2j}\sin\varphi)}{ka_{2j}\sin\varphi} - a_{2j-1}^2 \cdot \frac{J_1(ka_{2j-1}\sin\varphi)}{ka_{2j-1}\sin\varphi} \right] e^{-i\omega\Delta\tau_{2j,2j-1}}, \tag{2}$$

where $r_a = \sqrt{r^2 + z^2}$ is the distance from the centre of the array to the field point, $\varphi = \mathrm{arctg}(r/z)$, ρ_0 is the density of the liquid medium, ω is the angle frequency, and $\Delta\tau_{2j,2j-1}$ is the controlled time delay of the jth element. The radiation field of the annular phased array is calculated by Eq. (2) in numerical simulation in this study.

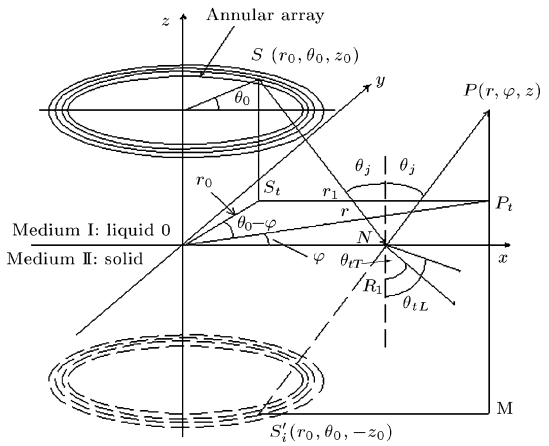


Fig. 1. The reflection on a solid–liquid interface of focused acoustical field excited by an annular phased array.

When the focused acoustical field of the annular phased array propagates to the solid–liquid interface, the reflection wave should be generated. As shown in Fig. 1, the reflection field φ_r in the liquid and the transmission fields (compressional wave φ_t and shear wave ψ_t) in the solid can be all written as follows according to the form of the radiation field given by Eq. (1):

$$\varphi_r = ik \sum_{j=1}^N e^{-i\Delta\phi_j} \iint_{s_j} ds \int_0^{\pi/2-i\infty} e^{ik\cos\theta z_0} \cdot J_0(kr_1\sin\theta) e^{ik\cos\theta_r z} V_{ll}\sin\theta d\theta,$$

$$\varphi_t = ik \sum_{j=1}^N e^{-i\Delta\phi_j} \iint_{s_j} ds \int_0^{\pi/2-i\infty} e^{ik\cos\theta z_0} \cdot J_0(kr_1\sin\theta) e^{-ik_{2L}\cos\theta_{tL} z} W_{ll}\sin\theta d\theta,$$

$$\psi_t = ik \sum_{j=1}^N e^{-i\Delta\phi_j} \iint_{s_j} ds \int_0^{\pi/2-i\infty} e^{ik\cos\theta z_0} \cdot J_0(kr_1\sin\theta) e^{-ik_{2T}\cos\theta_{tT} z} W_{lt}\sin\theta d\theta, \tag{3}$$

where k_{2L} and k_{2T} are the wave numbers of the compressional and shear waves in the solid, respectively; V_{ll}, W_{ll} and W_{lt} are the weighting coefficients which can be determined by the boundary conditions on the solid–liquid interface.

The reflection field of the annular phased array on the solid–liquid interface can be calculated numerically by Eq. (3). However, it is inconvenient to calculate because of the computing efficiency and precision. If the distance from the field point to the transducer is much greater than the wavelength, the ray approach method[4] can be used to obtain the concise analytic reflection field. Here, only the result of the reflection acoustical field is given because of the limitation of the paper length,

$$\varphi_r = \sum_{j=1}^N e^{-i\Delta\phi_j} \iint_{s_j} \frac{e^{ikR_1}}{R_1} V_{ll}(\theta_j) ds, \tag{4}$$

where R_1 is the distance from the mirror image of the integral element ds about the liquid-solid interface to the field point, $V_{ll}(\theta_j)$ is equal to the reflection coefficient of a plane wave propagating to the solid–liquid interface with the incident angle θ_j. It can be found that the reflection field is similar to the direct field from the mirror imaginary imaging of the annular array about the solid–liquid interface.

We design an annular phased array with eight elements. The inner and outer radii of each element are shown in Table 1. This is an equal-area-element annular transducer with working frequency of 0.3 MHz. The areas of each element are the same. Thus the acoustical fields, which are excited by the same electric signal from each element to the field point, are relatively approximate. Then, the annular phased array is connected to the digital transmission and collecting system to perform experimental measurements. A sine pulse with 30 periods is used to excite each element.

First, the experiment about the radiation field excited by the annular phased array is carried out. Figure 2 gives the acoustical field distribution along the axial and lateral directions when the focal length F (the distance from the centre of the array to the focus) is equal to 80 mm and 100 mm respectively. The real and plus lines represent the numerical simulation and experimental results. It can be seen from Fig. 2 that the experimental characteristics along the lateral distribution at the focal plane are in good agreement with the numerical simulation ones, especially in the main lobe parts. The width of the main lobe does

not change as the focus changes. The amplitudes of the lobes nearby the main lobe slightly increase as the focus increases. It can also be found that the forms and changing tendencies of the axial distributions of the theoretical and experimental results are also the same. However, the position of the maximum amplitude in the axis distribution of the theoretical result is not the same as that of the experimental result. There is a definite distance between them. Although some errors exist in the experiments, further investigation should be conducted.

Table 1. Parameters of the fabricated annular phased transducer.

Serial number	1	2	3	4	5	6	7	8
Inner radius (mm)	5	14.40	20.05	24.65	28.72	32.45	35.95	39.28
Outer radius (mm)	13.07	18.75	23.25	27.45	31.18	34.65	37.95	41.23

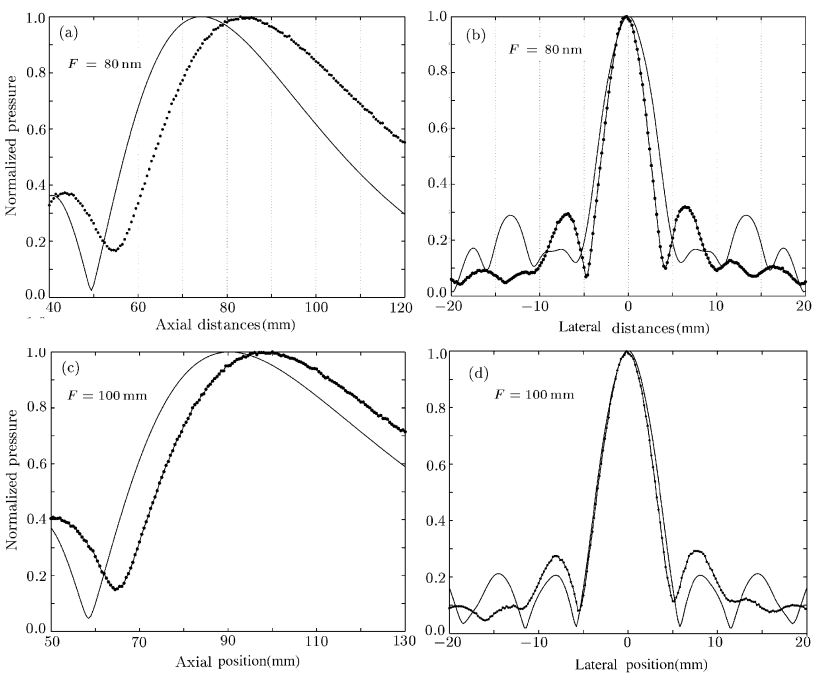


Fig. 2. The radiation acoustical field distribution along the axial and lateral directions of the annular phased array. The solid line and the circles represent the numerical simulation and experiment results, respectively. (a) Axial distribution, focal length $F = 80$ mm; (b) lateral distribution in the focal plane, $F = 80$ mm; (c) axial distribution, $F = 100$ mm; (d) lateral distribution in the focal plane, $F = 100$ mm.

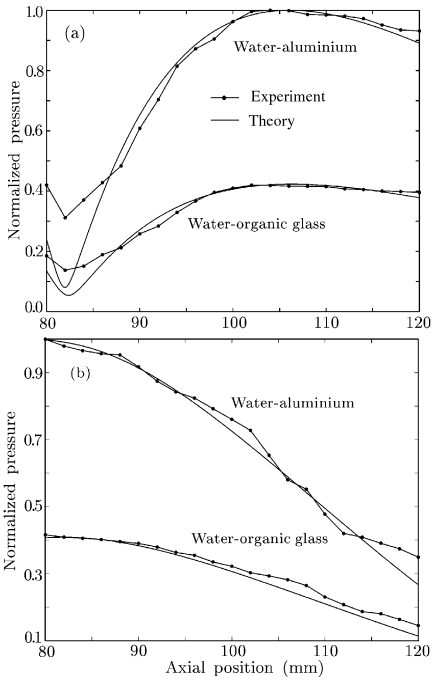


Fig. 3. The reflection acoustical field distributions. The abscissa represents the distances between the transducer and the reflection interface. (a) Focal length $F = 100$ mm; (b) dynamic focusing reflection acoustical field. The radiation field always focuses on the interface.

Then, the experiments of the reflection field measurement are conducted. Figure 3(a) depicts the reflection field of the annular phased array on the solid–liquid interface when the pre-designed focal length is equal to 100 mm. The abscissa represents the distances between the transducer and the reflection interface, and the y axis represents the normalized amplitude of the received wave. The receiver is located at the centre of the annular array. The real and the rectangle lines represent the theoretical and experimental results, respectively. Clearly we can see that both the matches are very well. When the distance between the transducer and the interface equals to the focal length of 100 mm, the acoustical reflection wave is highest. When the distance varies around the focal length, for example, from 95 mm to 110 mm, the reflection wave varies slightly. Also, it can be noticed that for different solid–liquid reflection interface, the reflection pattern varies greatly. It is found that the reflection at organic glass-water interface is greatly different that on aluminium–water interface. It is possible for us to evaluate some acoustic characteristics, such as the reflection coefficient, of the interfaces with the relative amplitude change of the reflection wave amplitude.

We alter the time delay of each annular element and let the radiation field always focus on the interface when the distance between the transducer and the interface changes. That is to say, the dynamic focusing is realized. Figure 3(b) gives the dynamic focusing reflection field when the distance between the transducer and the interface changes. We can see that the reflection field decreases as the distance increases. This is just what we expected.

With the maximum amplitude and its emergence

time of the reflection wave, we can acquire information of the acoustical parameters of the reflection interface and the distances between the transducer and the reflection interface. To display this sense, we show the reflection result on an aluminium block with cracks in Fig. 4 that gives the real structure and the acoustic reflection amplitude imaging of the aluminium model. The wave reflects at the aluminium-water interface when the transducer is above the aluminium surface, and there is no reflection interface when the transducer is above the cracks. The real size and experimental size of the cracks in the aluminium block are shown in Table 2. It can be seen from Fig. 4 and Table 2 that the positions of the cracks with widths of 14, 12, 10, 8, 6, 4 mm are very clear and the crack sizes can be determined. However, the cracks with widths of 2 mm and 1 mm cannot be distinguished because the working frequency is too low.

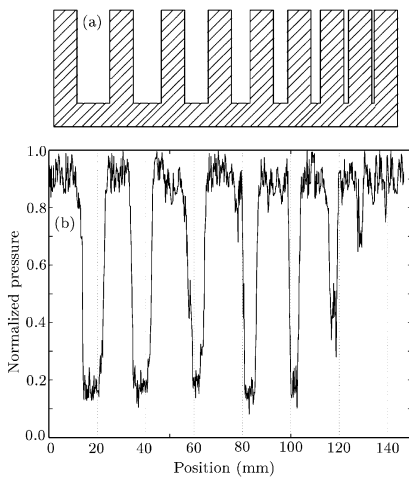
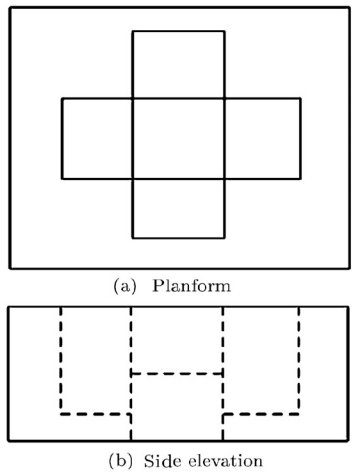


Fig. 4. The model of the aluminium block with cracks (a) and its reflection amplitude image (b).



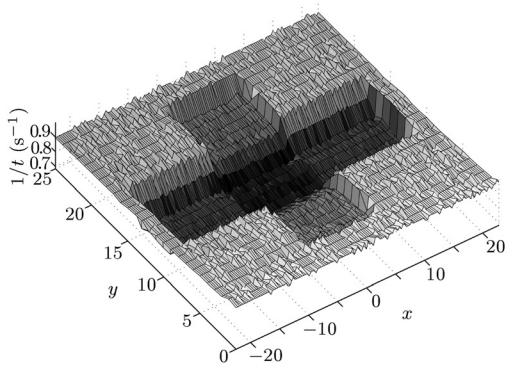


Fig. 5. The model of the three-edge aluminium block [(a) and (b)] and its reflection image (c).

Table 2. The size of the cracks in the aluminium model.

Real size (mm)	14	12	10	8	6	4	2	1
Experimental size (mm)	10	8	7	6	4.5	3	–	–

The reflection on a three-edge aluminium block is also measured. Figures 5(a) and 5(b) give the profile structure of the three-edge aluminium block. When the transducer moves above the three-edge aluminium block, the position of the reflection interface changes gradually. The arriving time of the reflection wave also varies gradually. According to the emergence time of the maximum amplitude of the reflection wave, we can obtain the distances between the transducer and the reflection interface. Figure 5(c) depicts the intuitive acoustic reflection image obtained by the emergence time of the maximum of the reflection waves. It clearly reveals the real surface structure of the three-edge aluminium block.

In this study, the acoustical radiation and reflection fields excited by a planar annular phased piezoelectric transducer are studied numerically and experimentally. The concise analytic representation about the radiation field excited by the annular phased array and its reflection field on a solid–liquid interface is theoretically obtained. The radiation and reflection acoustical fields are also measured in the ultrasonic experiments.

It is demonstrated that the reflection field reaches the highest when the focus is on the interface. With the maximum amplitude and its emergence time of the reflection wave, we can obtain the distances from the transducer to the reflection interface and other information about the interface. By the transmission-collection system and electric controlling system, the annular phased array can realize dynamic focusing and give accurately the imaging of the reflection interface.

This study lays a theoretical foundation for acoustic BHTV in practice although further study should be carried out in our next works.

References

[1] Jeremy A B et al 2004 *IEEE Trans. Ultrason. Ferroelectric. Freq. Control.* **51** 1010
[2] Lai P X, Zhang B X and Wang C H 2005 *Acoust. Technol.* **24** 339 (in Chinese)
[3] Maki V et al 1991 *SPWLA 32 Annual Logging Symposium* (Midland, Texas, 16–19 June 1991) paper HH
[4] Brekhowskikh L M 1985 *Waves in Layed Media* (Beijing: Academic Press) (in Chinese)
[5] Qian S Y 2003 *Appl. Acoust.* **22** 11 (in Chinese)
[6] Li J et al 2003 *Transaction of Shangxi Normal University (Natural Science Version)* **31** 28 (in Chinese)
[7] Ying C F 1993 *Ultrasonics* (Beijing: Academic) (in Chinese)
[8] Liu C 1999 *M.S. Thesis* (Institute of Acoustics, Chinese Academy of Sciences)
[9] Lai P X 2005 *M.S. Thesis* (Institute of Acoustics, Chinese Academy of Sciences)